Materials Today: Proceedings 70 (2022) 113–118

Contents lists available at ScienceDirect

Materials Today: Proceedings

journal homepage: www.elsevier.com/locate/matpr

Process map generation of geometrically uniform beads using support vector machine

Nowrin Akter Surovi *, Gim Song Soh

Singapore University of Technology and Design (SUTD), 8 Somapah Rd, Singapore 487372, Singapore

ARTICLE INFO

Article history:
Available online 16 September 2022

Keywords:
Additive manufacturing
Process Parameters Map
Machine learning
Bronze
Stainless Steel

ABSTRACT

In Wire Arc Additive Manufacturing (WAAM), weld beads are deposited layer-by-layer to form the final part. Thus, having geometrically non-uniform beads will lead to voids in the final printed part, which will significantly impact its overall quality and mechanical strength. The uniformity of beads depends on the proper choice of process parameters, namely the torch speed and wire feed rate. However, it is impossible to print all different combinations of these parameters to model the bead accurately, as printing them is expensive and time-consuming. Therefore, in this paper, we propose building a process map based on the probability that a weld bead is geometrically uniform using support vector machine. Experiments are carried out on the Bronze and Stainless Steel material datasets. The results show that the generated process map co-relates well with that of a manual quantization approach.

Selection and peer-review under responsibility of the scientific committee of The International Conference on Additive Manufacturing for a Better World.

1. Introduction

Wire Arc Additive Manufacturing (WAAM) is a direct energy deposition process that uses wire as feedstock and an electric arc as a power source to build 3D metallic components using a motion system [1]. The components are built by depositing overlapping weld beads in a layer-by-layer fashion [2]. Recently, WAAM is becoming popular because of its low capital cost, low buy-to-fly ratio, high deposition rate, and friendly to environment [3–7]. There are many approaches to building a WAAM system, and the common approach was to use a computer-controlled robotic system equipped with a welding power source, a welding torch, and a wire feed system.

Despite the above-mentioned advantages, there are challenges in the WAAM process that needs to be overcome in order for it to be used as a viable process. This includes print fusion defects, low tolerance to process variation, lack of design rules, lack of methods for qualification, etc. Furthermore, using different combinations of process parameters, diverse processing conditions can also generate beads of different quality. The print quality in WAAM is hard to predict and control due to its high sensitivity to process variability. Therefore, it is important to build an accurate process map to facilitate the qualification and certification of the print process to ensure the part is printed with a performance of up to a repeatable level [8]. Typically, such map is generated based on manual observation of the bead flow, which is labelled based on defects such as hump and scallop, incomplete toe fusion, etc. To the best of the authors' knowledge, there still does not exist a systematic approach to generating such a map. In this paper, we seek to address this and focus on building a process map based on the probability that a weld bead is geometrically uniform using support vector machine. The goal is to construct a process map where it can be used to avoid non-uniform weld bead prints as they create void or porosity in the final printed product [9].

Here we investigate the use of two types of dominant process parameters for WAAM such as torch speed (v_t) and wire feed rate (v_w) to generate the process map. The advantages of our proposed approach are many. First, it helps us predict the quality of beads based on their uniformity. Second, it gives a mapping relationship between process parameters and final part qualities. Third, it can reduce the number of experiments required to achieve a cost-effective and efficient development of AM parts over a wide range of materials [10]. Last, it shows machine learning can provide a practical methodology to optimize the process parameters of AM technologies [10].

* Corresponding author.
E-mail addresses: nowrin0102@gmail.com, surovi_akter@mymail.sutd.edu.sg (N.A. Surovi), sohgimsong@sutd.edu.sg (G.S. Soh).

https://doi.org/10.1016/j.matpr.2022.08.557
2214-7853/
Selection and peer-review under responsibility of the scientific committee of The International Conference on Additive Manufacturing for a Better World.

2. Experimental setup, data collection, and dataset labeling

2.1. Experimental setup

All the experiments were conducted on the robotic Wire Arc Additive Manufacturing (WAAM) system located at the Singapore University of technology and Design (SUTD). As shown in Fig. 1 (a), the system consists of a robot manipulator (ABB IRB1660ID), a welding power source (Fronius TPS 400i) equipped with a welding torch (Fronius WF 25i Robacta Drive), and a gantry robot made up of three linear rails (PMI KM4510) powered by three servos (SmartMotor SM34165DT) with a 2D laser scanner (Micro-Epsilon scanCONTROL 2910–100) attached. The gantry system is controlled to move the laser scanner in 3D space to measure point clouds of the printed layer's surface.

2.2. Data collectionss

We printed 50 weld beads using bronze (ERCuNiAl) wires and 52 weld beads using stainless steel (ER316LSi) wires for different combinations of torch speed and wire feed rate onto a substrate, as shown in Fig. 1(b). The length of each bead printed is around 10 cm. The torch speed and wire feed rate for our experiments range from [3,10] mm/s and [3,8] m/min respectively for bronze, and [3,15] mm/s and [3,6] m/min respectively for stainless steel.

The printed bead's height (h), width (w), and area (A) were measured using a 2D laser scanner. We filtered the scanner data using a moving average filter and extracted the weld bead's toe points from the second derivative of the filtered data. Based on our gantry measurement system resolution, the number of scan lines for each bead is 50 (for some beads, it is 49). Hence, we further segment each bead into 50 (or 49) segments for training and testing purposes.

2.3. Dataset labeling

We divided defective and non-defective beads based on how non-uniformity it is. When the geometrical shape of the printed bead is uniform, we refer to it as non-defective, and when the bead shape is less uniform, we refer to it as defective. Here we use a "Combined Root Mean Square Error (RMSE)" of a bead segment width, height, and area to measure its uniformity [9]. The smaller the combined RMSE, the better the quality of the bead. This is defined by.

$$y = \frac{width_{RMSE} + height_{RMSE} + \sqrt{area_{RMSE}}}{3} \tag{1}$$

3. Methodology

Our proposed process parameter map divides non-defective (good) and defective (bad) beads based on their probability. The procedure for generating such a process parameter map is as shown in Fig. 2 and it consists of two parts. First, we train a two-parameter sigmoid function based on the SVM classifier function $f(x)$ and the various segment labels $Y = [y_i]$. Next, we used the learned sigmoid function to obtain the probability for a particular set of process parameters $x_i = (v_t, v_w)$ that will yield a geometrically uniform bead to generate the process map.

3.1. Training/Learning

The non-linear support vector machine (SVM) function used for our classifier is.

$$f(x) = \sum_{j=1}^{n} y_i \alpha_i k(x_j, x) + b \tag{2}$$

whose inputs $X = [x_i]$ are a matrix of features which consists of the process parameters (v_t, v_w). The inputs Y are a matrix of associated labels and is computed based on a bead uniformity as described by Eq (1). Here, we use Radial Basis Function (RBF).

$$k(x_j, x) = exp - (\gamma ||x - x_j||^2)$$

as the kernel to our classifier function. For our application, we choose $\gamma = 0.1$. The coefficients α_i and b are the parameters to be trained based on the obtained datasets.

Next, we convert the classifier output into probabilities by Platt scaling [11]. To do so, we use two parameters sigmoid function, which takes the output of the classifier f_i and converts them into probabilities. The probability function is given by the sigmoid function of the form.

$$p_i = \frac{1}{1 + exp(1 + f_i A + B)} \tag{3}$$

where $f_i = f(x_i)$. The coefficient A and B can be found by minimizing the negative log-likelihood of training data, which is also known as cross-entropy loss of the form $\sum y_i log(p_i) - (1 - y_i) log(1 - p_i)$.

3.2. Prediction

After learning an optimal A^* and B^* for the learned sigmoid function, the same sigmoid function Eq (3) is used for probability prediction based on a set of process parameters x_i. To find the probability p_i for a certain set of process parameter x_i that generates a good bead, Eq. (4) is used.

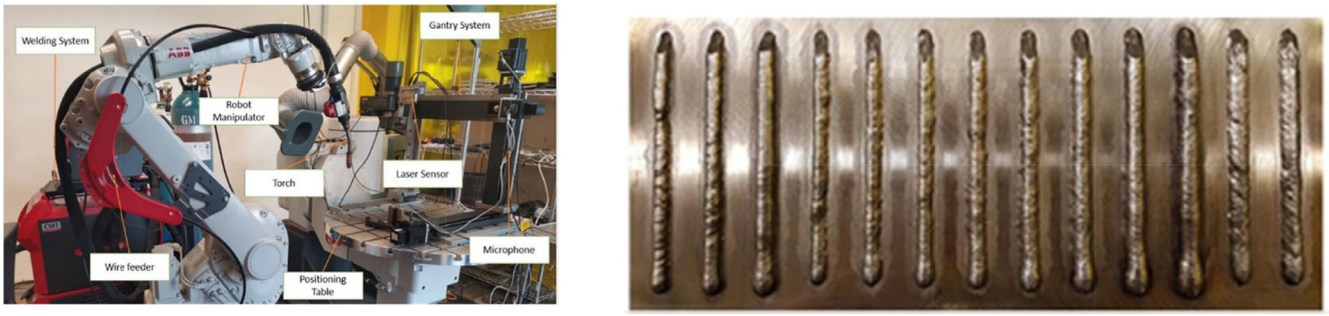

Fig. 1. (a) Experimental setup of SUTD WAAM for Data collection (b) Illustration of the Bronze weld beads plate.

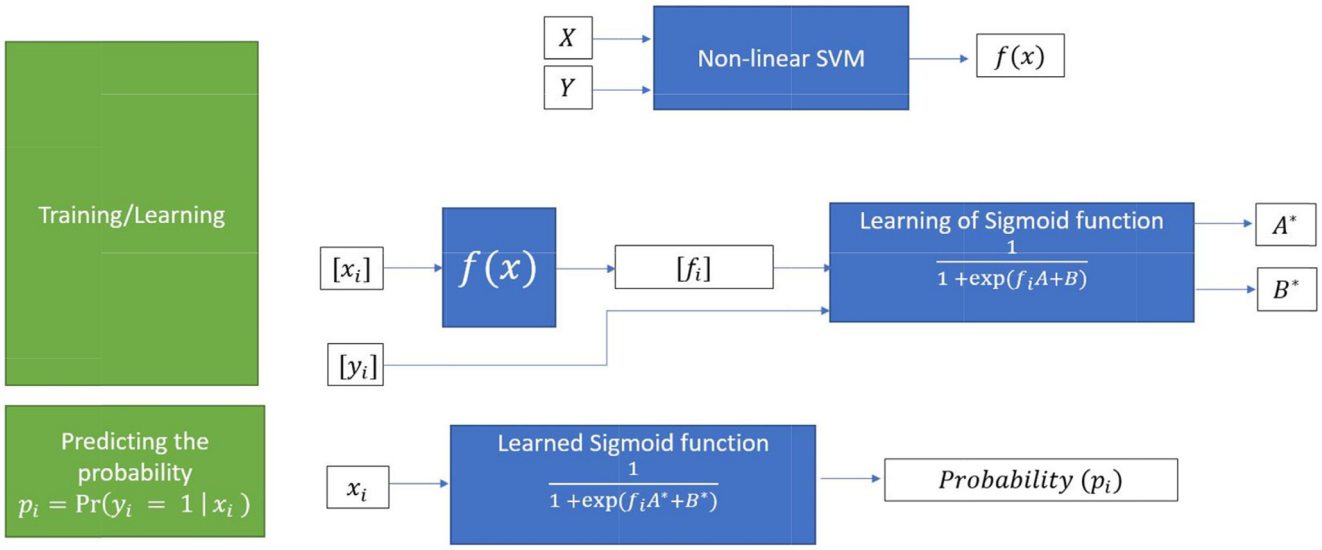

Fig. 2. Our procedures for process parameter map generation.

$$p_i = P(y_i = 1|x_i) \tag{4}$$

4. Process map generation and performance evaluation

4.1. Training and testing datasets

The training dataset we used for stainless steel is n = 1950 (based on 39 beads), and the testing dataset is 650 (based on 13 beads). Similarly, for bronze, the training dataset used is n = 1950 (39 beads), and the testing dataset is 539 (11 beads).

4.2. Process map generation

We plot the process parameters map $\boldsymbol{x_i} = (\boldsymbol{v_t}, \boldsymbol{v_w})$ based on its probability to produce a good bead for both the Bronze and Stainless Steel materials. They are as shown in Fig. 3. This plot is predicted from the learned Sigmoid Function as denoted by Eq. (4). The brown region indicates a high probability that the set of process parameters can form a good bead, while the blue region indicates a low probability that it will form a bad bead. The white region indicates that the probability is 0.5, meaning in that region of process parameters, both good and bad beads can form with equal probability.

4.3. Benchmarking with manual quantization

To validate our generated process map results, we have a WAAM expert performing manual quantization of the process parameter map based on her experience. The results are as shown in Fig. 4.

Fig. 5 shows both Figs. 3 and 4 superimposed on each other. We observe that the process map for both stainless steel and bronze matches well based on the human quantization process. Therefore, we can conclude that the generated process parameter map based on our approach is consistent with the current approach. However, for our approach, we have the advantage of additional information as compared to the current approach, such as a prediction of the quality of the beads at the boundary region.

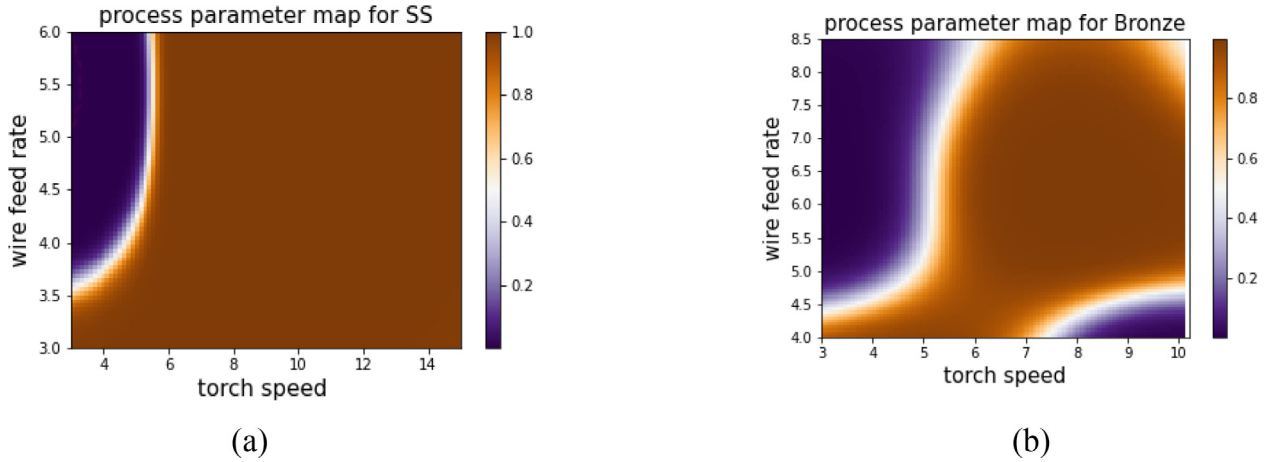

Fig. 3. Process parameter map generation using SVM for (a) Stainless steel (SS) and (b) Bronze.

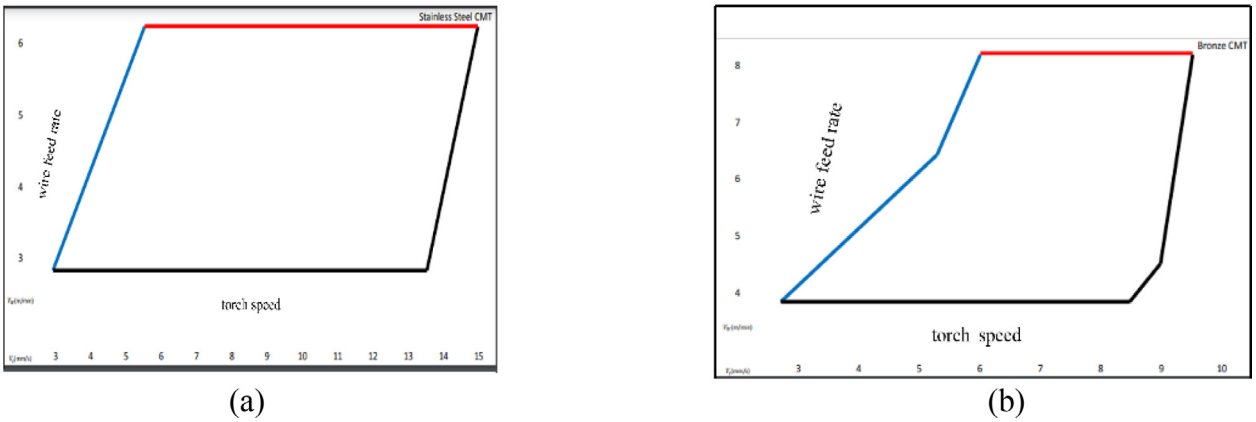

Fig. 4. Expert manual quantization Process parameter map for (a) Stainless steel (SS) and (b) Bronze.

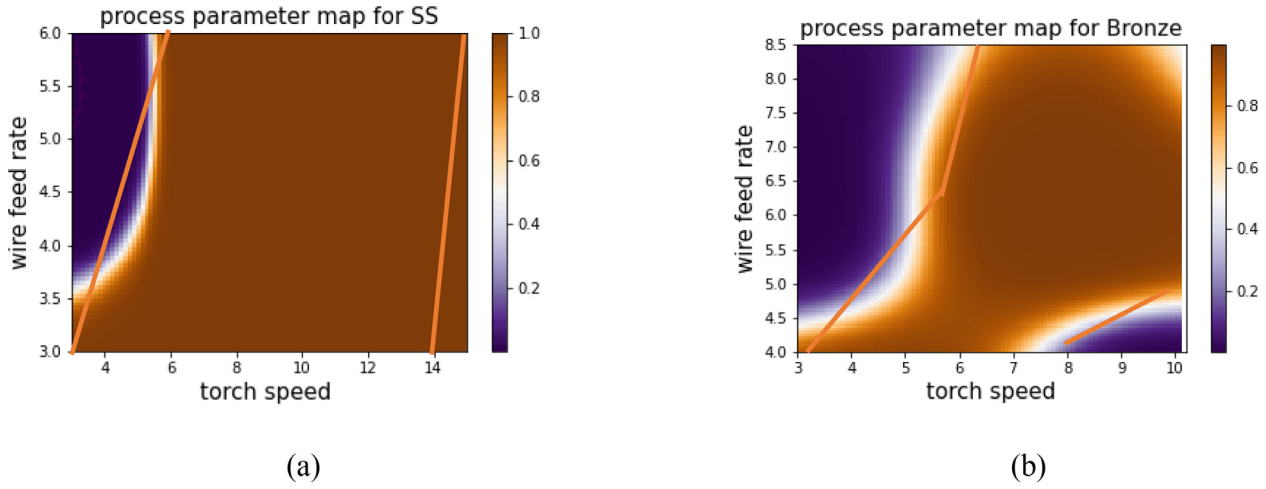

Fig. 5. Comparison of two Process parameter maps for (a) Stainless steel (SS) and (b) Bronze.

4.4. Performance evaluation

Now we quantify the performance of our learned non-linear SVM model based on the testing accuracy and confusion matrix. To perform this, we expand our training features parameters and include geometric parameters like the bead height (h), width (w), or area (A) for training and testing. Eight combinations of features, as shown in Table 1, including those that we used to generate the process map, are evaluated to understand their resulting accuracy.

Table 1 shows the results of the testing accuracy of our model for the two datasets (Stainless and Bronze). From the table, we can see that the testing accuracy is the same for all combinations of inputs features for stainless steel at 92 %. However, for bronze, the testing accuracy varies from 68 % to 76 %, depending on which combinations of inputs features are used.

Table 2 shows the confusion matrix based on the different features used. From the results, we can observe that our model can predict 550 good bead segments correctly from out of the 600 good stainless steel testing datasets for all combinations of features. Also, it is worth noting that the model can predict all the 50 bad stainless steel segments correctly. However, for bronze, we get different confusion matrices based on the combinations of features used. The best feature combination is $X = (v_t, v_w, h, w)$, and the model can only pick out 294 good segments correctly out of the 343 good bronze testing datasets, and 120 bad segments out of the 196 bad bronze testing datasets.

Table 1
Different combinations of inputs give different testing accuracy.

Input Features (X)	Testing accuracy (SS)	Testing accuracy (B)
torch speed wire feed	92 %	72 %
torch speed wire feed height	92 %	73 %
torch speed wire feed width	92 %	72 %
torch speed wire feed area	92 %	69 %
torch speed wire feed height width	92 %	76 %
torch speed wire feed height area	92 %	69 %
torch speed wire feed width area	92 %	68 %
torch speed wire feed height width area	92 %	72 %

Table 2
Different combinations of inputs give different confusion matrix.

Features (Stainless Steel)			True		Features (Bronze)			True	
			Good	Bad				Good	Bad
torch speed wire feed	Predicted	Good	550	0	torch speed wire feed	Predicted	Good	343	147
		Bad	50	50			Bad	0	49
torch speed wire feed height	Predicted	Good	550	0	torch speed wire feed height	Predicted	Good	294	92
		Bad	50	50			Bad	49	104
torch speed wire feed width	Predicted	Good	550	0	torch speed wire feed width	Predicted	Good	342	145
		Bad	50	50			Bad	1	51
torch speed wire feed area	Predicted	Good	550	0	torch speed wire feed area	Predicted	Good	342	164
		Bad	50	50			Bad	1	32
torch speed wire feed height width	Predicted	Good	550	0	torch speed wire feed height width	Predicted	Good	294	76
		Bad	50	50			Bad	49	120
torch speed wire feed height area	Predicted	Good	550	0	torch speed wire feed height area	Predicted	Good	294	115
		Bad	50	50			Bad	49	81
torch speed wire feed width area	Predicted	Good	550	0	torch speed wire feed width area		Good	342	168
		Bad	50	50			Bad	1	28
torch speed wire feed height width area	Predicted	Good	550	0	torch speed wire feed height width area	Predicted	Good	294	101
		Bad	50	50			Bad	49	95

5. Conclusion

We have proposed a method to construct the process parameter map for WAAM based on the uniformity of bead geometry using support vector machine. This method enables a systematic approach to generate the process map based on a probability approach. A label was proposed to measure a bead uniformity based on the RSME of its width, height, and area. Experiments were conducted on Stainless Steel and Bronze material, and we found that the process map generated based on our proposed approach co-relates well with a human quantization approach. We also quantify the performance of our learned non-linear SVM model based on the testing accuracy and confusion matrix.

CRediT authorship contribution statement

Nowrin Akter Surovi: Writing – original draft, Conceptualization, Methodology, Software, Validation, Investigation. **Gim Song Soh:** Writing – review & editing, Validation, Visualization, Supervision.

Data availability

The data that has been used is confidential.

Declaration of Competing Interest

The authors declare the following financial interests/personal relationships which may be considered as potential competing interests: Soh Gim Song reports financial support was provided by A*STAR AME IAF-PP, Singapore. Nowrin Akter Surovi reports financial support was provided by Ministry of Education, Singapore.

Acknowledgments

The authors gratefully acknowledge the support of the A*STAR AME IAF-PP, Singapore; Grant number A19E1a0097.

References

[1] T.A. Rodrigues, V. Duarte, R. Miranda, T.G. Santos, J. Oliveira, Current status and perspectives on wire and arc additive manufacturing (WAAM), Materials 12 (7) (2019) 1121.
[2] A. Busachi, J. Erkoyuncu, P. Colegrove, F. Martina, J. Ding, Designing a WAAM based manufacturing system for defence applications, Procedia Cirp 37 (2015) 48–53.
[3] D. Ding, Z. Pan, D. Cuiuri, H. Li, A practical path planning methodology for wire and arc additive manufacturing of thin- walled structures, Rob. Comput. Integr. Manuf. 34 (2015) 8–19.
[4] F. Xu, V. Dhokia, P. Colegrove, A. McAndrew, S. Williams, A. Henstridge, S.T. Newman, Realisation of a multi-sensor framework for process monitoring of the wire arc additive manufacturing in producing ti-6al-4v parts, Int. J. Comput. Integr. Manuf. 31 (8) (2018) 785–798.
[5] L. Yuan, Z. Pan, D. Ding, F. He, S. van Duin, H. Li, W. Li, Investigation of humping phenomenon for the multi-directional robotic wire and arc additive manufacturing, Rob. Comput. Integr. Manuf. 63 (2020) 101916.
[6] B. Wu, Z. Pan, D. Ding, D. Cuiuri, H. Li, J. Xu, J. Norrish, A review of the wire arc additive manufacturing of metals: proper- ties, defects and quality improvement, J. Manuf. Processes 35 (2018) 127–139.
[7] C. Xia, Z. Pan, J. Polden, H. Li, Y. Xu, S. Chen, Y. Zhang, A review on wire arc additive manufacturing: monitoring, control and a framework of automated system, J. Manuf. Syst. 57 (2020) 31–45.
[8] Byeong-Min Roh et al. "Ontology-based process map for metal additive manufacturing". In: Journal of Materials Engineering and Performance 30.12 (2021), pp. 8784–8797

[9] N. A. Surovi, A. G. Dharmawan, G. S. Soh. A study on the acoustic signal based frameworks for the real-time identification of geometrically defective wire arc bead, in: International Design Engineering Technical Conferences and Computers and Information in Engineering Conference, Vol. 85383, American Society of Mechanical Engineers, 2021, p. V03AT03A003.

[10] Kenta Aoyagi et al. "Simple method to construct process maps for additive manufacturing using a support vector machine". In: Additive manufacturing 27 (2019), pp. 353–362

[11] J. Platt, Probabilistic outputs for support vector machines and comparisons to regularized likelihood methods, Adv. Large Margin Classifiers 10 (3) (1999) 61–74.